4.1.2 Extent of reduction determined by pulse O_2-titration.

At 673 K oxygen titration of some of the catalysts was tried as an alternative method to TPR for determination of the extent of reduction. The temperature was chosen because this is the "standard" temperature for oxygen titration of reduced cobalt catalysts using the volumetric method as described by Bartholomew /73/. This method is also reported by several other works /32,35,36,37,38/. At 673 K the oxidation of the reduced metal phase is assumed to be complete, and the product is assumed to be Co_3O_4 /35/. The results from pulse O_2 titration and from TPR are shown in Table 4-8 below. The TPR spectra in Figure 4-12 are from a platinum promoted cobalt catalyst, comparing reduction for 16 hours at 623 K with reduction in a standard TPR run up to 1173 K. Table 4-9 contains literature data /7,35,38/ showing the degree of reduction of alumina supported cobalt catalysts found by different methods. They are compared with the results from the present work.

Table 4-8. Degree of reduction[a] (%) of catalysts found by pulse O_2 titration at 673 K after reduction for 14 hours at 623 K, and by TPR during a corresponding reduction.

Catalyst	Pulse O_2 titration[a]		TPR	
	Co	CoX[b]	Co	CoX[c]
Co/Al_2O_3A	52	52	40	40
$Co1.0Pt/Al_2O_3A$	84	79	88[e]	83[e]
$Co1.0Pt^*/Al_2O_3A$[d]	82	78		
$Co1.0Re/Al_2O_3A$	89	78		

[a] The reoxidation of reduced cobalt is assumed to be complete after oxygen pulsing at 673 K. Then the degree of reoxidation of the catalyst is considered equal to the degree of reduction. The degree of reoxidation is calculated from the oxygen consumption compared to the total amount of cobalt on the catalyst, assuming Co_3O_4 being formed during reoxidation.

[b] The amount of oxygen needed to complete oxidation of Pt and Re, to PtO_2 and Re_2O_7 is subtracted from the total oxygen consumption before calculation of degree of reduction of cobalt.

[c] The amount of hydrogen needed to complete reduction of Pt and Re, from PtO_2 and Re_2O_7 is subtracted from the total hydrogen consumption before calculation of degree of reduction of cobalt.

[d] * denotes that a chloride containing platinum precursor is used.

[e] The catalyst used is $Co1.0Pt/Al_2O_3B$, calcined at 573 K.

Table 4-8 shows that the extent of reduction calculated from pulse O_2 titration is in rather good agreement with the reduction extent calculated during a TPR with 2 K/min up to 623 K. However, a difference (52 % versus 40%) is observed for Co/Al_2O_3A, where O_2 titration gives the largest reduction extent. This difference can be suggested to be due to the measurement method in TPR, because the hydrogen consumption during a possible, very slow reduction under isothermal conditions (623 K, 16 hours) can be difficult to measure. But on the other hand, the hydrogen consumption measured during a further heating to 1173 K with 10 K/min after the "standard reduction", corresponds to a total degree of reduction of 95%. This indicate that most of the hydrogen consumed during the isothermal period is recognized.

For the platinum promoted catalyst the difference in measured reduction extent between the two methods is only 4 %. In this case the O_2 titration shows the lowest reduction extent. But it must be noted that the promoted catalyst investigated in TPR is calcined at a lower temperature (573 K) than the others (673 K). Investigation of the effect of calcination temperature (Chapter 4.1.1.1) has shown a decreasing extent of reduction with increasing calcination temperature. It could therefore be guessed that with the same calcination temperature, the reduction extent from TPR would have been a little lower than measured by O_2 titration.

O_2 titration at 673 K shows that all the promoted catalysts are reduced to the same extent. Small differences observed in oxygen consumption between the promoted catalysts disappear when subtracting the amount of oxygen needed to reoxidation of the noble metal. The coincidence in extent of reduction for all the promoted catalysts is also in agreement with trends found by TPR (Chapter 4.1.1.3 - 4.1.1.5).

Altogether the comparisons made above show that there is just small differences between the two methods in calculation of reduction extent. Results obtained with one method in the present laboratory are then comparable with results obtained with the other method.

When comparing the TPR spectrum of a platinum promoted catalyst calcined at 573 K and reduced for 16 hours at 623 K with the TPR spectrum of the same catalyst reduced in a programmed run up to 1173 K as in Figure 4-12, the same peaks are seen in both spectra. The

degree of reduction calculated for Co1.0Pt/Al_2O_3B when reduced in a programmed run with 10 K/min. up to 1173 K is 82 (± 5 % uncertainty because of the large nitrate peak). A reduction temperature program of 2 K/min up to 623 K and then constant temperature for 16 hours gives a degree of reduction on 88 %.

Table 4-9 shows that reduction extent in the same range are found by volumetric O_2-titration /35,38/. Reuel and Bartholomew /35/ found an extent of reduction of 34% for an uncalcined 10%Co/Al_2O_3 catalyst reduced at 648 K. Reduction extent found by XPS are not directly comparable with the results from the other methods. But the XPS results reported by Chin and Hercules /7/ also showed reduction extent in the range 25 - 45 % for Co/Al_2O_3 catalysts. Besides the results confirm that the extent of reduction decreases with increasing calcination temperature.

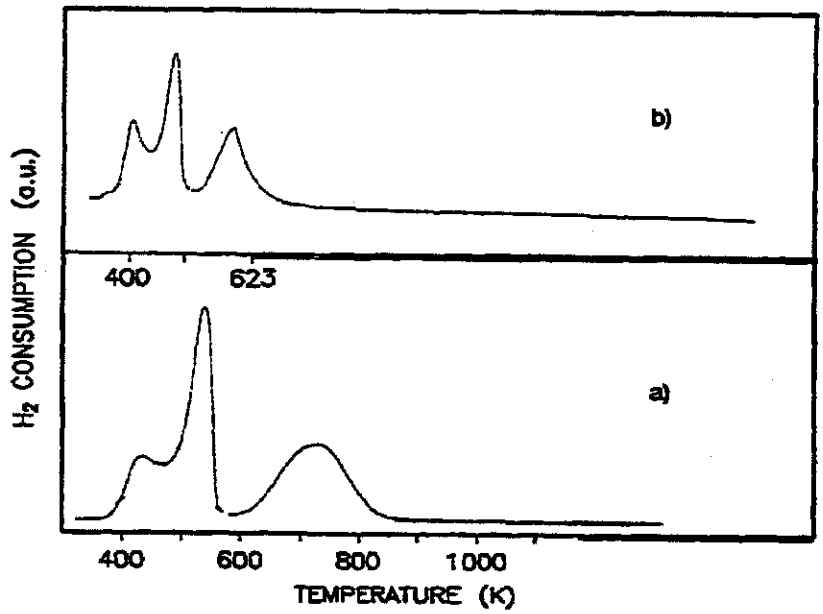

Figure 4-12. TPR spectra of Co1.0Pt/Al_2O_3B at different temperature programming. a) 10 K/min, 293 to 1173 K, b) 2 K/min from 293 to 623 K, and then at constant temperature 623 K for 16 h.

Table 4-9. Comparison of different ways of calculating the degree of reduction of cobalt catalysts prepared by impregnation of alumina with cobalt nitrate.

Catalyst	Calcination	Reduction	Method	Degree of reduction (%)	Reference
8%Co/Al_2O_3	673 K, 5 h	673 K, >4 h	XPS	35	Chin and Hercules /7/
8%Co/Al_2O_3	873 K, 5 h	673 K, >4 h	XPS	25	Chin and Hercules /7/
16%Co/Al_2O_3	673 K, 5 h	673 K, >4 h	XPS	43	Chin and Hercules /7/
10%Co/Al_2O_3	773 K, 24h	623 K, 4 h	Volumetric O_2-titration	17	Lee, Lee and Ihm /38/
10%Co/Al_2O_3	None	648 K, 20 h	Volumetric O_2-titration	34	Reuel and Bartholomew /35/
15%Co/Al_2O_3	None	648 K, 20 h	Volumetric O_2-titration	44	Reuel and Bartholomew /35/
8.7%Co/Al_2O_3A	673 K, 2 h	623 K, 16 h	TPR	40	This work, Table 4-8
8.7%Co/Al_2O_3B	573 K, 2 h	623 K, 16 h	TPR	36	This work, Fig. 4-8 and Table 4-2
8.7%Co/Al_2O_3A	673 K, 2 h	623 K, 14 h	Pulse O_2-titration	52	This work, Table 4-8

4.1.3 Volumetric chemisorption of H_2 and CO

The results presented below are obtained after the same pretreatment of all the catalysts: Heating from room temperature to 623 K in 150 ml pure hydrogen per minute and gram of catalyst, at a heating rate of 2 K/min, and then reduction at 623 K for 14 -16 hours. Variations in reduction time between 14 and 16 hours are not considered to be critical for the comparison of the results. XPS studies /7/ and TPR spectra (the present study) show that most of the reduction occurs during the first 4 - 5 hours. An example of an adsorption isotherm and the calculation of the corresponding dispersion are given in Appendix 3. In addition to the figures shown below the results from all the adsorption measurements are tabulated in Appendix 4.

In the figures below the difference in gas uptake between the first and the second isotherm is, due to common practice, called "irreversible" adsorption, while the gas uptake measured by the second isotherm is called "reversible" adsorption. However, measurements have shown that the amount of "reversible" adsorption is increasing with the evacuation time between the uptake of the two isotherms. Therefore it must be realized that all adsorption in principle is reversible. With use of the same evacuation time in all experiments, differences in "irreversible" adsorption can indicate changes in the strength of the adsorption. Due to this, the term "strong" and "weak" adsorption will be used in the further discussion.

The hydrogen uptake is expressed as [mol H / mol Co_{tot}], and the CO uptake is expressed as [mol CO / mol Co_{tot}].

4.1.3.1 Effect of calcination temperature

Strong and weak hydrogen adsorption were measured for cobalt catalysts calcined at three different temperatures; 573, 648 and 673 K. The results are shown in Figure 4-13.

In Figure 4-13 it is shown that the total hydrogen uptake decreases slightly with increasing calcination temperature. The same trend is not clear for the strongly adsorbed part of the H_2 uptake. For the two catalysts calcined at 573 and 673 K, 70 - 75 % of the total hydrogen

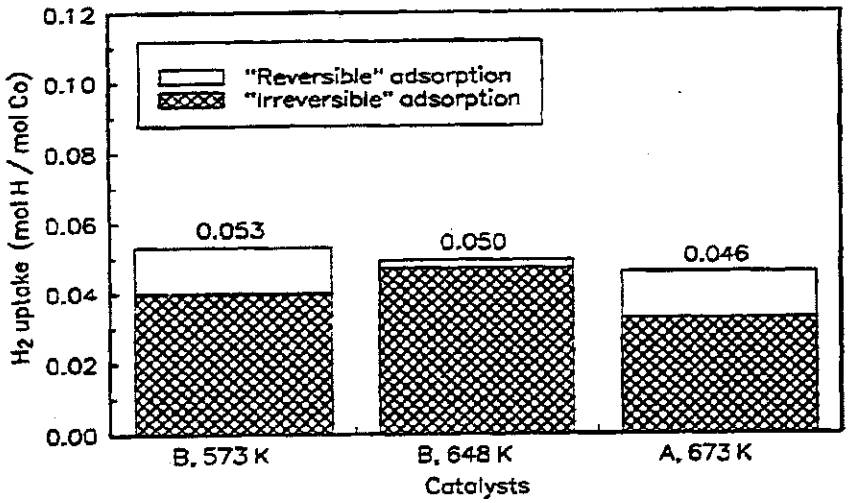

Figure 4-13. H_2 uptake at 298 K on Co/Al_2O_3 catalysts calcined at different temperatures and reduced at 623 K in flowing H_2 for 16 hours. Support A and B.

uptake is measured to be adsorbed strongly. For the catalyst calcined at 648 K the same part is 95 %.

In Figure 4-13 results for catalysts made from two different γ-Al_2O_3 supports are shown. However, the specifications from the manufacturers are very similar for the two supports. In addition, the pore size distribution and surface area for the calcined cobalt catalysts were measured by nitrogen adsorption/mercury penetration and BET, respectively. The results are nearly the same for catalysts made from the two different supports (Appendix 5). It is therefore not probable that support effects will affect the adsorption results.

The TPR peaks representing reduction of Co_3O_4 (Figure 4-1) showed a shift to higher temperature, while the hydrogen consumption was constant, with increasing calcination temperature of the catalysts. This was suggested (Chapter 4.1.1.1.) to be caused by a higher degree of sintering of Co_3O_4 at higher calcination temperatures /137/. The decrease in hydrogen adsorption with increase in calcination temperature (Figure 4-13) can then also be

suggested to be caused by larger cobalt particles, leading to lower dispersion. Data in Table 4-9 show that the catalyst calcined at 673 K is reduced to a slightly higher extent compared to the catalyst reduced at 573 K. A decrease in reduction extent can therefore not explain the observed decrease in hydrogen adsorption.

The total hydrogen uptake on 8.7%Co/Al_2O_3 shown in the present work is about 1.5 times higher than reported by Bartholomew and Reuel /81/ for similar catalysts. This differences can be due to different catalyst pretreatment procedures. The fraction of weakly adsorbed hydrogen is in good agreement in the two works.

4.1.3.2 Effect of platinum and rhenium promotion

Hydrogen adsorption on catalysts with different platinum loadings is shown in Figure 4-14, and CO adsorption on the same catalysts is shown in Figure 4-15. A comparison of the effect of promotion with platinum and rhenium on H_2- and CO adsorption is also done. Hydrogen adsorption on catalysts with 1 wt% rhenium and platinum addition is shown in Figure 4-16,

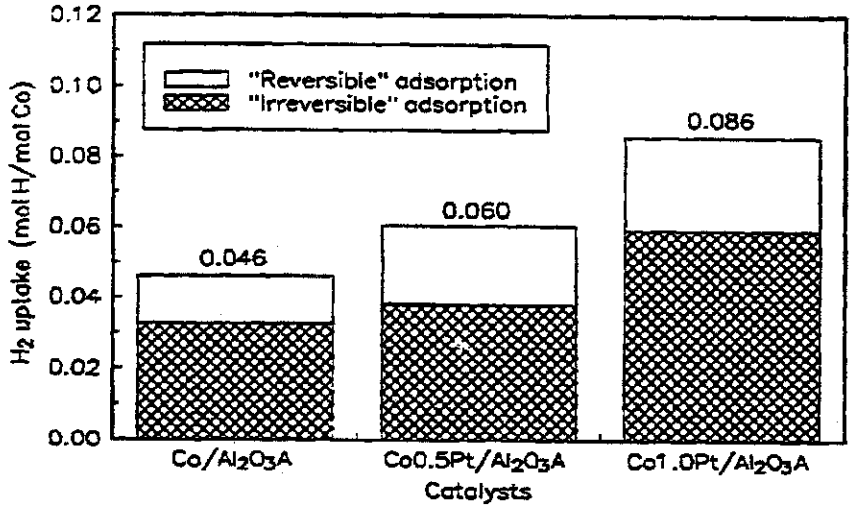

Figure 4-14. H_2 adsorption on catalysts with various platinum loading. Chloride free platinum precursor and calcination temperature 673 K.

and CO adsorption on these catalysts is shown in Figure 4-17. Figure 4-18 shows the ratio between the amount of CO and H adsorbed on different catalysts.

The hydrogen adsorption is increasing with increasing platinum amount (Figure 4-14). The hydrogen uptake on Co0.5Pt/Al_2O_3A is nearly one and a half time the hydrogen uptake on Co/Al_2O_3A, while the adsorption on Co1.0Pt/Al_2O_3A is nearly twice the adsorption on Co/Al_2O_3A. A slightly larger part of the hydrogen is weakly adsorbed on the promoted catalysts.

The CO adsorption, shown in Figure 4-15, is also increasing with increasing platinum amount. But the increase in the CO adsorption is larger compared to the increase in hydrogen adsorption. The CO uptake on Co1.0Pt/Al_2O_3A is 0.065 mol CO/mol Co, which is nearly three times the uptake on Co/Al_2O_3A. On Co0.5Pt/Al_2O_3A the CO adsorption is 0.042 mol CO/mol Co.

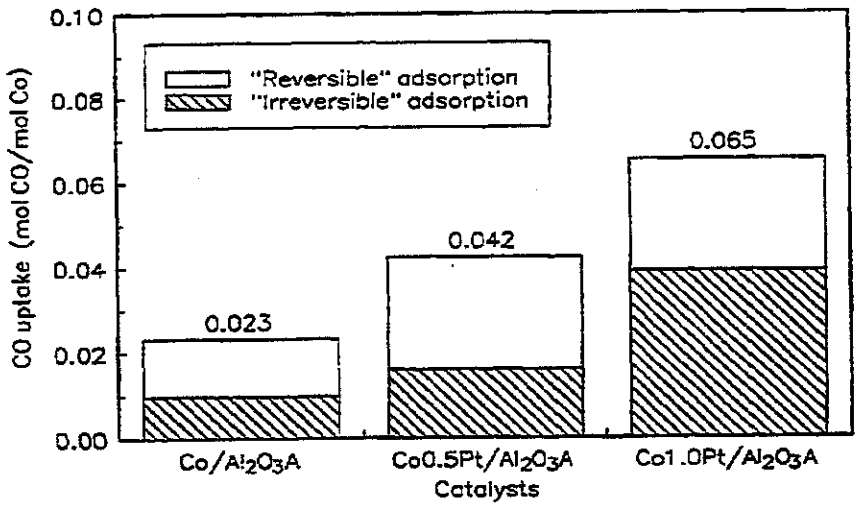

Figure 4-15. CO adsorption on catalysts with various platinum loading. Chloride free platinum precursor and calcination temperature 673 K.

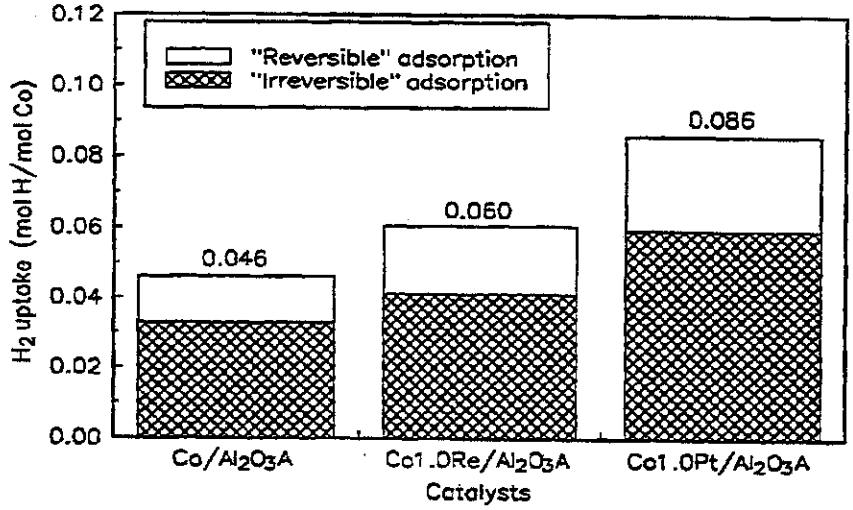

Figure 4-16. **H_2 adsorption on cobalt catalysts promoted with 1 wt% chloride free Pt and Re. Calcination temperature 673 K.**

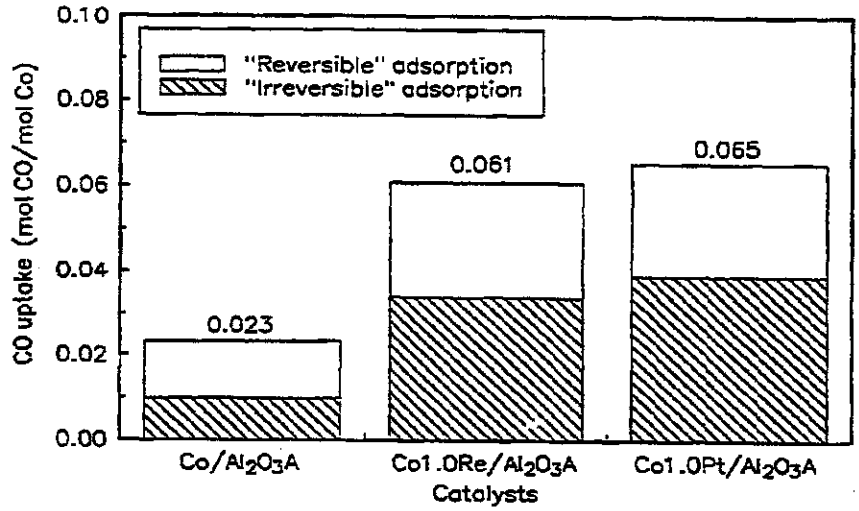

Figure 4-17. **CO adsorption on cobalt catalysts promoted with 1 wt % chloride free Pt and Re. Calcination temperature 673 K.**

When comparing hydrogen adsorption on a pure cobalt catalyst with catalysts promoted with approximately 1 wt % of rhenium or platinum (Figure 4-16) an increase in adsorption is observed for both the promoted catalysts. But the increase in hydrogen adsorption on the rhenium promoted catalyst is less than half of the increase in hydrogen adsorption on the platinum promoted catalyst. The hydrogen uptake on Co1.0Re/Al_2O_3A is 0.060 mol H/mol Co and equal to the hydrogen uptake on Co0.5Pt/Al_2O_3A.

In Figure 4-17 the CO adsorption on rhenium and platinum promoted catalysts are compared. It is shown that there is no pronounced difference between the CO uptake on the two promoted catalysts. Both show a large increase in CO adsorption compared to the pure cobalt catalyst. The amount of strongly adsorbed CO is also nearly the same for the two promoted catalyst.

Figure 4-18 shows that the ratio between CO and H generally is higher for weakly adsorbed gases than for strongly adsorbed. The CO:H ratio increases for the catalysts in the order

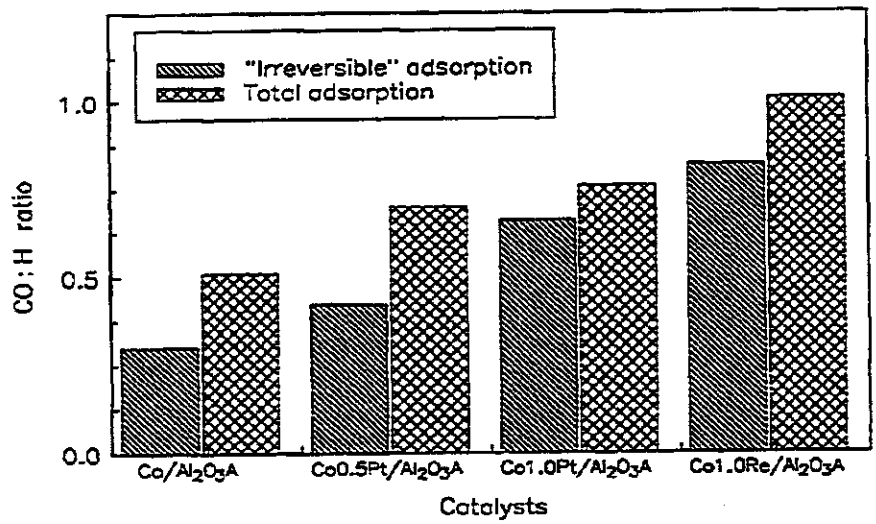

Figure 4-18. The ratio between CO and H uptake on different catalysts calcined at 673 K and reduced in situ at 623 K for 16 hours.

Co1.0Re > Co1.0Pt > Co0.5Pt > Co.

For Co1.0Re/Al_2O_3A the total amount of CO adsorbed is the same as the total amount of H atoms adsorbed. For Co/Al_2O_3A the amount of CO adsorbed is half the amount of H atoms adsorbed.

The increase in H_2 and CO adsorption with increased platinum loading has several possible explanations.

I) Increased degree of cobalt reduction due to platinum promotion as seen from the TPR-results in Figure 4-8 will give higher degree of available metallic cobalt surface, and thus higher H_2 and CO adsorption.

II) Platinum is known /86.107.110.124/ to adsorb both hydrogen and CO at room temperature. If it is assumed that platinum exists as a separate phase or in an alloy behaving much like platinum, then the gradual increase in H_2 and CO adsorption with increasing platinum loading could also be due to adsorption on the platinum.

III) It is well known /111/ that hydrogen is able to spill over from well dispersed platinum to the support, and this will increase the measured amount of hydrogen.

IV) Spillover from reduced platinum to cobalt oxide could also be assumed as a possible reason for increased adsorption on promoted catalysts /47/.

V) Bartholomew et al. /45/ have reported results indicating that CO and H_2 are able to spill over from cobalt metal crystallites to the support. The higher degree of reduction of the oxidic cobalt layer on surface on the promoted catalyst gives an increased interface between reduced cobalt and support (or unreduced $CoAl_2O_4$) surface. This increased interface makes the spillover mechanism more possible.

VI) If platinum does not exist as a separate phase, but rather as an alloy with the surface phase of cobalt, there will be interactions between platinum and cobalt, which may

increase the gas adsorption capacity of cobalt compared to cobalt in a separate phase.

No single explanation among I) - VI) is necessarily the correct one: combinations of two or several effects are possible. It should be noted that:

I) It is not necessarily a linear correlation between the degree of reduction and the amount adsorbed. At least two possibilities can be suggested to cause changes in the cobalt dispersion for the promoted catalysts compared to the unpromoted: a) Cobalt-platinum interactions can modify the cobalt particle size. b) Two or several "particle size regimes" can exist as a result of reduction of different cobalt oxide phases. In addition to the different surface area for particles of different sizes, the adsorption behavior can vary due to different degree of interactions between the alumina support and the reduced cobalt.

II) Platinum can be assumed to be 100 % dispersed, and a Pt:H ratio can be assumed to be 1:1 as indicated in literature data /106,107,108/. The hydrogen consumption corresponding to platinum adsorption is subtracted from the total hydrogen consumption,

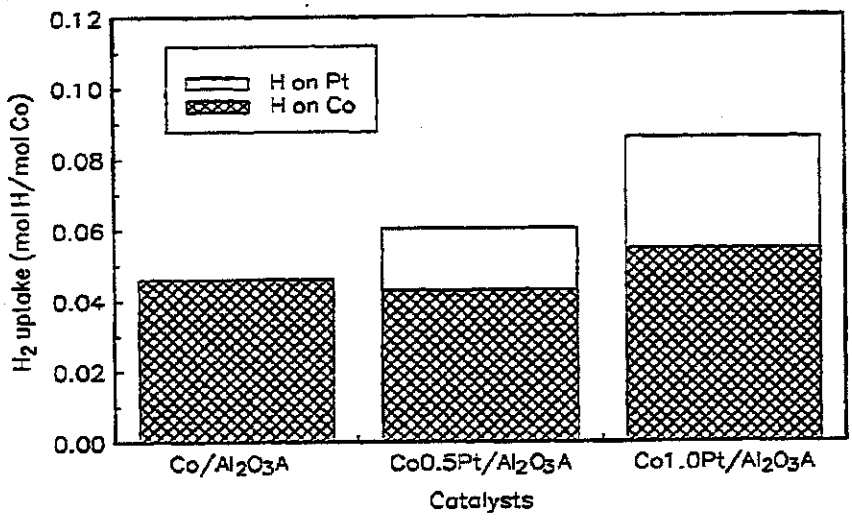

Figure 4-19. H_2 adsorption on cobalt catalysts with various platinum loading. 100 % dispersion of Pt, and a Pt:H ratio of 1:1 assumed.

and the remaining fraction of hydrogen is then assumed to be adsorbed on cobalt. The result from these calculations is shown in Figure 4-19 above. It is seen that with these assumptions the hydrogen adsorption on cobalt remains almost constant with increasing platinum loading. However, recently published works /113,105/ indicate that the platinum reduction on alumina supported monometallic Pt /105/, or bimetallic PtCo /113/, catalysts is incomplete after one hour calcination and reduction at 770 K, due to strong Pt-Al_2O_3 interactions for some part of the platinum. The catalysts used in this study are reduced at 623 K. In addition, platinum dispersion on $Pt/ZnAl_2O_4$ catalysts is dependent of platinum loading /114/, and when the Pt loading is above 0.5 wt% particle formation is suggested to take place. A similar situation could be imagined for platinum on Al_2O_3. 100 % dispersion of platinum is therefore not probable, and accounting for hydrogen adsorption on platinum in $CoPt/Al_2O_3$ will be less important than indicated in Figure 4-19.

As seen from the TPR runs of prereduced catalysts in Figure 4-8, both the rhenium and the platinum promoted catalyst are almost completely reduced after 16 hours at 623 K. The difference in hydrogen adsorption between these two catalysts is therefore not assumed to be due to a different degree of reduction. One reasonable explanation of this phenomena is that rhenium do not /126/ adsorb, or adsorb very small amounts /127/ of hydrogen at room temperature. The excess of hydrogen adsorbed on the platinum promoted catalyst compared to the rhenium promoted catalyst, could then be due to hydrogen adsorption on platinum as indicated in point II) and III) above.

The CO adsorption data in Figure 4-17 shows that the difference between platinum and rhenium promoted catalysts seen for hydrogen adsorption disappears for the CO adsorption. It could therefore be suggested that rhenium is able to adsorb CO, but not hydrogen. These differences could indicate that rhenium and platinum exist, at least partly, as pure metal particles that are responsible for some of the increased CO adsorption relative to the pure cobalt catalyst.

Bartholomew /58/ has studied cobalt catalysts extensively and concludes with increased reversibility of hydrogen adsorption with decreasing extent of reduction. The trend seen in

Figure 4-14 is not in agreement with this conclusion. The promoted catalysts are reduced to higher extent and simultaneously show higher degrees of reversibility. When Bartholomew varied the degree of reduction, the metal loading was not constant. In this study the cobalt loading is constant. From the TPR data it is known that the oxidic cobalt layer on surface is reduced on the promoted catalysts. When reduced, this phase may have adsorption behavior different from the larger Co_3O_4 particles, giving a weaker adsorption of hydrogen. The disagreement could also be due to the platinum present. If hydrogen adsorbs on platinum as well as on cobalt (point II), the adsorption on platinum might be weaker than on cobalt. The total effect of this could be increased degree of weak adsorption. Increased hydrogen adsorption on the support on the promoted catalysts could also cause the increased "weakly adsorbed" fraction (point III). Platinum may also change the physical properties of cobalt, resulting in more weak adsorption at low temperature (point VI).

The lower CO:H ratio for strongly adsorbed gases seen in Figure 4-18 compared to the same ratio for total amount of adsorbed gases is a result of the large amounts of weakly adsorbed CO (40 - 60 %). A weak CO adsorption is found to take place on Al_2O_3 /45/, and some part of the weakly adsorbed CO may be on the support. Lapidus et al. /79,80/ found three different adsorption states (I - III) for CO adsorption on 10 % Co/Al_2O_3, and only one of these was assigned to reduced cobalt metal. Adsorption state I and III were also found for the unreduced catalyst. The most weakly bound form of adsorbed CO, form I, is suggested to correspond to adsorption on cobalt-aluminum compounds or on the support itself. Form III is suggested to represent CO adsorption on Co_3O_4. It could also from these results be suggested that weakly adsorbed CO is not only on cobalt metal, but also on unreduced cobalt phases or on the alumina support.

The low $(CO:H)_{irreversibel}$ ratio on Co/Al_2O_3A is not consistent with literature data /35,38,81/ for 10 % Co/Al_2O_3. This ratio is typically reported to be in the range 1.1 - 1.4 in contrast to 0.25 in the present study. The difference is due to both higher (50 %) hydrogen adsorption and much lower (1/3) irreversible CO adsorption in this investigation. The difference between the literature data and the results presented here could be due to differences in the measurement methods. The evacuation time between the first and the second isotherm is important for determining the amount of weakly adsorbed gas. In addition, the literature data

were measured by the desorption (decreasing pressure) method. It should also be mentioned that differences in pretreatment and degree of reduction could be an important factor, causing the differences observed in the adsorption behavior.

It could only be speculated in reasons for the low CO:H adsorption ratio: One possibility is hydrogen spillover, another is the existence of bridge bound CO molecules at the measurement conditions, which would change the adsorption stoichiometry from 1:1 to 1:2.

Both linearly and bridge bound CO were found by Zaitsev et al. /82/ and by Fredriksen /128/ on 10 % Co/Al_2O_3 using IR even though other authors /83,84,85/ report predominantly linearly bound CO on silica and alumina supported cobalt. Johnson et al. /87/ found that CO adsorbs both molecularly and dissociatively on Co overlayers on tungsten. Dissociation takes place on two types of sites: A Co/W interfacial site at submonolayer coverage of Co/W(100) and Co/W(110), and on the pseudomorfic monolayer of Co/W(100). Nørskov /116/ reported that CO adsorbs non-dissociatively on cobalt metal. But it was also stated that open surfaces are usually more reactive in dissociating simple gas molecules than the close packed ones. Then there might be some chance for dissociative CO adsorption on the reduced surface phase on the promoted catalysts.

The small difference in CO and H_2 adsorption for the cobalt rhenium catalyst compared to the platinum promoted catalysts, is partly explained by the absence of hydrogen adsorption on rhenium. A reason for the increased CO:H ratio for the promoted catalysts (both Pt and Re) compared to the unpromoted could be the nature of the cobalt surface phase that is reduced to a higher degree in the catalysts with a promoter (as seen in Figure 4-8). It is reported that decoration with the alumina support leads to diminished H_2 adsorption, while the CO adsorption is unaffected by this /40/. Then it can be suggested that for the surface phase on the promoted catalysts the intimate contact to the support gives a decoration of the reduced cobalt. Another possibility is hydrogen spillover from reduced cobalt to the unreduced oxidic layer on the unpromoted catalysts.

It could on the other hand also be suggested that if the CO:H ratio on platinum and rhenium is much larger compared to cobalt, this could cause the observed increase in the CO:H ratio.

Vannice /86,124/ found a $(CO:H)_{total}$ ratio = 0.6 on 1.2 % - 1.75 % Pt/Al_2O_3 at room temperature. This is in the same range as obtained on the cobalt-platinum catalysts in the present study (Figure 4-18), and could therefore partly explain the increased CO:H ratio.

4.1.3.3 Effect of chloride

Figure 4-20 shows H_2 adsorption on catalysts with different platinum loadings made from a chloride containing platinum precursor. It is seen that these catalysts adsorb somewhat less hydrogen than the monometallic cobalt catalyst. The hydrogen adsorption on these catalysts is accordingly not dependent of platinum loading in the same way as it was on chloride free platinum promoted catalysts.

The nearly constant hydrogen adsorption with increasing platinum loading when using chloride containing platinum precursor was unexpected from the TPR results. TPR investigations of platinum promoted catalysts with and without chloride containing precursor (Figure 4-9) showed that chloride to some extent changed the promotional effect of platinum

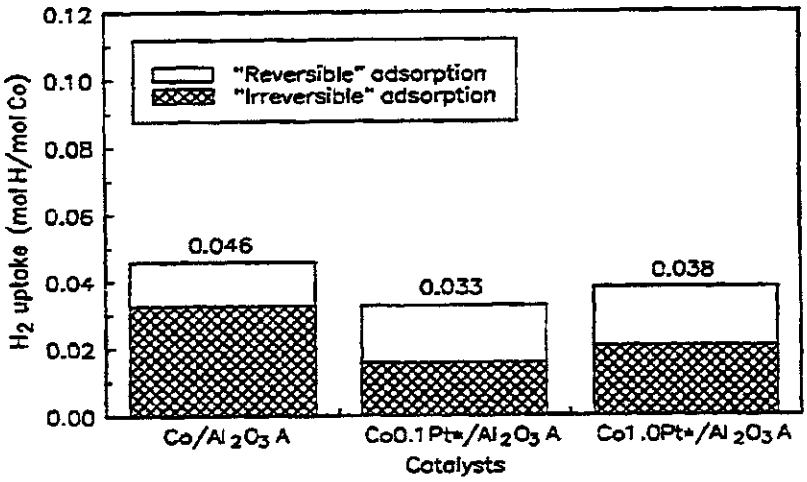

Figure 4-20. H_2 adsorption on catalysts with various platinum loading. Chloride containing platinum precursor and calcination temperature 673 K.

on cobalt reduction. However, the heavy reducible cobalt surface phase was reduced at lower temperature when promoted with chloride containing platinum precursor compared to chloride free platinum precursor. The two different platinum containing cobalt catalysts should therefore be expected to be reduced to nearly the same high extent after 14 hours at 623 K.

Oxychlorination of sintered platinum catalysts is known to enhance the dispersion of platinum /71/. This is supported from the temperature shifts observed in the TPR experiments in this study (discussion in Chapter 4.1.1.6). Also in view of this an increased hydrogen uptake should be expected on the chloride containing platinum promoted catalysts. As this not is the case there could be other chloride effects on the catalyst surface. Some of these effects could be:

I) The ion exchange of chloride ions with hydroxyl groups on the support giving lower degrees of hydrogen spillover from the platinum /65/ is mentioned earlier. Since it also is suggested that parts of the measured hydrogen adsorption on the chloride free platinum promoted catalysts are adsorbed on the support surface, it seems reasonable that some parts of the decreased hydrogen uptake could be due to chloride poisoning of the support.

II) Matzusaki et al. /50/ did suggest that chloride species cause agglomeration of the cobalt particles during reduction. This will give less cobalt surface available for hydrogen adsorption and reaction. Zsoldos and Guzci /113/ report XPS measurements indicating lower dispersion of Co_3O_4 on bimetallic 10 % $CoPt/Al_2O_3$ ($x_{Co} = 0.85$) compared to the dispersion of Co_3O_4 on monometallic cobalt samples. They suggest that platinum or chloride increases the particle size of Co_3O_4. The results presented in this study, showing different results for chloride containing and chloride free CoPt catalysts, support that chloride is responsible for the influence on the particle size.

III) It could be speculated in electronic effects of chloride on cobalt and platinum, giving less hydrogen adsorption. The H_2 adsorption is weaker on the chloride containing catalyst. This could be due to a $Co^{\delta+}$ caused by chloride.

IV) As will be shown in the next chapter, XRD measurements of reduced and in room temperature passivated catalysts showed that the chloride containing platinum promoted catalyst contains hexagonal cobalt metal, while the platinum and rhenium promoted catalysts without chloride contain cubic cobalt metal. This difference, resulting in decreased number of surface sites, could also be a part of an explanation for the decreased hydrogen adsorption on the chloride containing catalyst.

4.1.3.4 Dispersion and crystallite size

In catalyst studies it is for many purposes interesting to know the dispersion and the crystallite size of the active metal phase. The dispersion can be found by several different methods, and should ideally be independent of the measurement method. When disagreements between the dispersion calculated from measurements with different methods nevertheless appear, this often reflects the characteristic assumptions for a particular technique. An example of such assumptions is the adsorption stoichiometry. Hydrogen is in the calculations below assumed to be dissociativly adsorbed /107,108,109/, while CO is assumed to be associatively (linearly) adsorbed /116/.

With the elements of uncertainty linked with the adsorption on bimetallic catalysts, it is difficult from the adsorption data only to find the correct dispersion of the reduced cobalt phase that could be used for calculation of the turnover frequency in activity tests. However, two models that do not take into account spillover to the support could be suggested:

I) All the measured gas molecules or atoms are adsorbed on cobalt or a mixed cobalt/noble metal phase, active for the Fischer-Tropsch reaction.

II) The reduced, noble metal is 100 % dispersed and the amount of hydrogen or CO corresponding to adsorption on noble metal is subtracted from the adsorbed gas amount before calculating the dispersion on cobalt. (Rhenium is not assumed to adsorb hydrogen.)

Cobalt crystalline size can be calculated from adsorption data and from XRD measurements on calcined catalysts. When Reuel et al. /35/ calculated the particle size from adsorption data they assumed spherical particles of uniform size, and corrected for the unreduced amount of cobalt on the catalyst. The following equation were used to calculate the particle size (d):

$$d = \frac{6.59\ s}{\%D_r} \qquad (4\text{-}1)$$

where s - Site density in atoms/Nm^2

D_r - Dispersion, taking into account reduction extent

Surface site densities are a function of the crystal structure and the distribution of crystallographic planes /35/. Generally surface site densities are calculated from an equally weighted average of the planar densities for the most dense planes. For the face centered cubic cobalt (fcc) equally weighted average of the site densities for the (100), (110) and (111) planes was used in the calculation of s, and this gave 14.6 atoms/Nm^2. A weighted average of the site densities for the most dense planes of the hexagonal close packed cobalt (hcp) structure, namely 2x(001), 6x(100), 6x(110), gave a site density of 11.2 atoms/Nm^2 /35/.

Whether to use total or "irreversibly" amount of adsorbed gas for calculating the dispersion is not obvious. The presence of "weakly" adsorbed gas could indicate more than a monolayer of hydrogen or CO adsorbed, but also adsorption on several types of sites with different adsorption strength. In the first case use of only the "strongly" adsorbed gas will give the best estimate of dispersion. However, since the amount of the weakly adsorbed gas is varying with the time of evacuation between the measurements of the two adsorption isotherms, this size is not clear (Appendix 4). If the weakly adsorbed gas indicates different types of cobalt sites, the total gas amount is assumed to give the best estimate of number of adsorption sites on the surface.

Analysis of the line broadening based on the half-maximum width of the (111) peak in the XRD spectra gives the particle diameter from the Scherrer formula /70/:

$$d = \frac{K \cdot \lambda}{\beta \cdot \cos\theta} \qquad (4\text{-}2)$$

where K - Scherrer constant, 0.9
λ - wavelength, 1.5418 Å
ß - broadening of the diffraction line, B - 0.20
B - experimental line width
Θ - Bragg angle, 18.433

Table 4-10 shows calculations (not taking into account reduction extent) of cobalt dispersion (based on adsorption data reported in Chapter 4.1.3.2) on promoted and unpromoted cobalt catalysts. The two adsorption models suggested are used in the calculations of the dispersion. Figure 4-21 shows the XRD bands appearing from the same catalysts after calcination at 673 K, reduction at 623 K and passivation in O_2 at 298 K. Unfortunately, these XRD bands were too diffuse for calculating the particle size. Instead, XRD measurements of calcined, not reduced, catalysts were used to this purpose. Particle size (d) calculations from the H_2 chemisorption and XRD are compared in Table 4-12. The degree of reduction found from

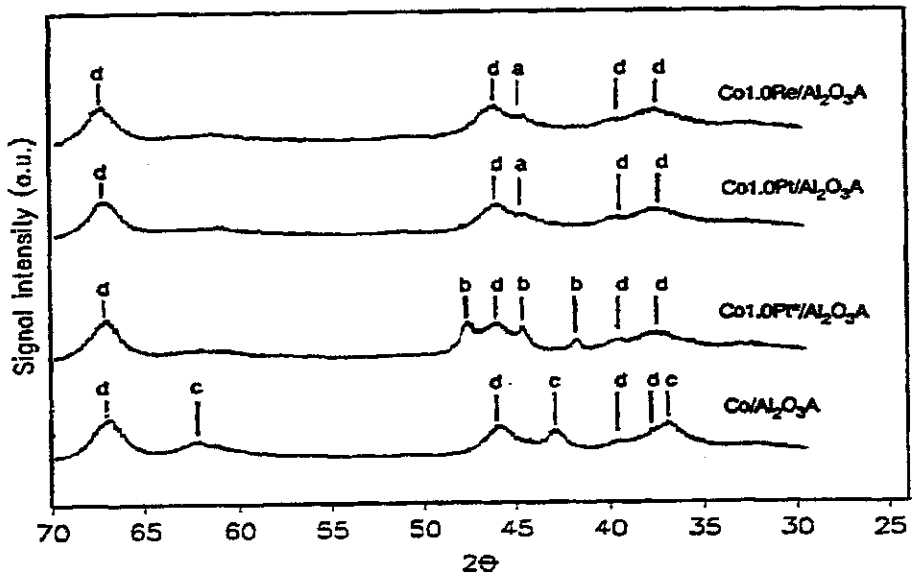

Figure 4-21. XRD analyses. Calcination at 673 K, reduction at 623 K for 16 h and passivation in O_2 at 298 K. a) Co(fcc): 44.19 b) Co(hcp): 47.42, 44.48, 41.59 c) CoO: 61.69, 42.99, 36.85 d) γ-Al_2O_3: 67.03, 45.86, 39.49, 37.60.

both TPR analysis and from O_2 pulse titration are used and the resulting particle sizes using Eq.4-1 and 4-2 are listed in the table. s = 14.6 atoms/Nm^2 is used for the Co, CoRe and the chloride free CoPt catalysts, while s = 11.2 atoms/Nm^2 is used for the chloride containing catalyst, based on the major cobalt crystalline phases found from XRD measurements of the reduced and passivated catalysts in Figure 4-21. Table 4-11 shows the O_2 consumption, expressed as "degree of reduction" (similar to Table 4-8), when pulsing O_2 on prereduced catalysts at 298 K.

Dispersion values from weakly adsorbed CO in Model II (Table 4-10) seem unreasonable because no adsorption is found to take place on reduced cobalt in two of the catalysts. The use of weakly adsorbed H_2 in Model II gives lower dispersion on the promoted catalysts than on the unpromoted catalyst. This does not agree with the higher extent of reduction for these catalysts, unless the reduced cobalt consists of larger crystallites compared to the cobalt on unpromoted catalysts. These calculations using the strongly adsorbed gas only, indicate that some part of the weakly adsorbed gas is on reduced cobalt sites and that the second metal is not 100 % dispersed. Due to this the total amount of adsorbed gas is chosen as the basis for the calculations of particle size.

Table 4-10. Cobalt metal dispersion from volumetric chemisorption data[a].

Catalyst	Dispersion from total adsorption (%)				Dispersion from "irreversible" ads. (%)			
	H_2 adsorption		CO adsorption		H_2 adsorption		CO adsorption	
	Mod.I[b]	Mod.II[c]	Mod.I	Mod.II	Mod.I	Mod.II	Mod.I	Mod.II
Co/Al_2O_3A	4.6	4.6	2.3	2.5	3.3	3.3	1.0	1.0
$Co0.5Pt/Al_2O_3A$	6.0	4.3	4.2	2.5	3.8	2.1	1.6	0
$Co1.0Pt/Al_2O_3A$	8.6	5.5	6.5	3.4	5.9	2.8	3.9	0.8
$Co1.0Re/Al_2O_3A$	6.0		6.1	1.7	4.1		3.4	0

[a] It is not taken into account the reduction extent.
[b] Model I): All the gas molecules or atoms are adsorbed on cobalt.
[c] Model II): The noble metal is 100 % dispersed and the amount of hydrogen or CO corresponding to adsorption on noble metal is subtracted from the adsorbed gas amount before calculating the dispersion on cobalt.

As discussed in connection with the adsorption data the assumption of only linearly adsorbed CO molecules could be uncertain. Table 4-10 shows that 1:1 CO adsorption stoichiometry gives consistently lower dispersion than hydrogen adsorption data. If only bridge bound CO is assumed, the dispersion will become higher than calculated from hydrogen adsorption. Bartholomew /142/ recommend H_2 adsorption for the calculation of dispersion because of the unknown CO adsorption stoichiometry. Reuel et al. /35/ found very good agreements of average crystallite diameters estimated from total hydrogen adsorption (assuming $H/Co_s=1$), XRD and TEM.

The data in Table 4-11 show that the catalysts are only partly reoxidized at 298 K, and a passivation of the outermost layers of the cobalt particles has most probably occurred. The oxygen consumption of the chloride free platinum and rhenium catalysts at 298 K is more than 6 times the oxygen consumption of the unpromoted catalyst. For the chloride containing platinum promoted catalyst the oxygen consumption is about 2.5 times the consumption of the unpromoted catalyst. At 673 K the oxygen consumption is higher in all cases and the reoxidation of the reduced cobalt was assumed to be complete.

Table 4-11. Degree of reduction[a] (%) of catalysts found by pulse O_2 titration at 298 K (passivation) after reduction for 14 hours at 623 K.

Catalyst	O_2 consumption		
	298 K, Co	298 K, CoX[b]	673 K, Co
Co/Al_2O_3A	5	5	52
$Co1.0Pt/Al_2O_3A$	32	27	84
$Co1.0Pt^*/Al_2O_3A$[c]	13	10	82
$Co1.0Re/Al_2O_3A$	31	20	89

a The oxygen consumption is expressed as the degree of reoxidation (reduction), calculated from the oxygen consumption compared to the total amount of cobalt on the catalyst, assuming Co_3O_4 being formed during reoxidation.

b The amount of oxygen needed to complete oxidation of Pt and Re, to PtO_2 and Re_2O_7 is subtracted from the total oxygen consumption before calculation of degree of reduction of cobalt.

c * denotes that a chloride containing platinum precursor is used.

Table 4-12. Comparison of cobalt dispersion (D) and particle size (d) found when using Esq. (4-1) and (4-2).

Catalyst	D'_{TPR}[a] (%)	D'_{O}[b] (%)	d_{TPR}[a] (nm)	d_{O}[b] (nm)	d_{XRD}[c] (nm)	d_{TEM}[d] (nm)
Co/Al_2O_3A	11.5	8.8	6.4	8.4	19	
$Co1.0Pt^*/Al_2O_3A$	4.6	4.9	21.0	19.7	20	
$Co1.0Pt/Al_2O_3A$	10.3	10.9	7.1	6.8	14	
$Co1.0Re/Al_2O_3A$	7.3	7.8	10.1	9.5	19	
$10\%Co/Al_2O_3$ /35/				9.7[e]		11/15

[a] Based on total adsorption of H_2, model I and reduction degrees found from TPR.
[b] Based on total adsorption of H_2, model I and reduction degrees found from pulse O_2 titration.
[c] Measurements on calcined, not reduced, catalysts (the Co_3O_4 phase).
[d] d_s/d_v, d_s= Surface mean diameter, d_v= Volume mean diameter.
[e] Based on total adsorption of H_2 and reduction degrees found from volumetric O_2 titration.

The XRD measurements reported in Table 4-12 are done on Co_3O_4 particles on not reduced catalysts. They show that the Co_3O_4 particle size is about the same (20 nm) for the four investigated catalysts, except for the chloride free CoPt catalyst, which has somewhat smaller (14 nm) particles than the other. The particle size of the reduced cobalt fraction calculated from the total H_2 adsorption is in the same range (6 -10 nm) for three catalysts. In this case the chloride containing CoPt catalyst has more than twice the size of the other. The size calculated for the Co/Al_2O_3 catalyst is in good agreement with the size found by Reuel et al. /35/ for a similar 10 % cobalt catalyst.

From TPR it is clear that for the promoted catalysts the oxidic cobalt surface layer is reduced after 16 hours at 623 K. This phase is assumed to be well dispersed. However, the particle size calculation shows constant, or larger, particle size of the reduced cobalt on the promoted catalysts. The points III) and IV) in the discussion of the adsorption behavior with and without platinum addition (spillover from platinum to the support or to oxidic cobalt, Chapter 4.1.3.2), shows that the possibility for overestimation of dispersion is largest for the promoted catalysts. If this is effect is present, then the real particle size of the promoted particles is

even larger than shown in Table 4-12. Two different possible explanations for the surprising calculated particle sizes could be suggested:

I) Surface Co^{2+} and Co^{3+} ions agglomerate during the reduction and forms Co^0 particles with nearly the same size as the Co^0 particles formed from Co_3O_4.

II) Co^0 particles with two different size regimes exists on the surface:
   a) Relatively large particles generated from Co_3O_4.
   b) Well dispersed, small particles with high surface area, but with apparently low dispersion due to strong interactions with the support, generated from the oxidic surface layer.

When discussing these two possibilities, the result from XRD measurements of the reduced and passivated catalyst must be mentioned:

The cobalt in the different catalysts exists in different phases after reduction and passivation in oxygen. In the unpromoted cobalt catalyst CoO is found, while in the chloride free platinum and rhenium promoted catalysts cobalt metal is present in cubic (fcc)orientation. The chloride containing platinum promoted catalyst contains a hexagonal (hcp) cobalt structure.

Cobalt is known /35.115/ to exist as hcp structure at temperatures below 723 K and as fcc structure at temperatures above 723 K. But when the particle size is small, the stable structure is fcc, even at temperatures below 723 K. This support that the chloride containing catalysts really has larger particles than the other. In this case the first explanation seems plausible, and the larger particles could be due to chloride caused agglomeration of cobalt as suggested by Marzusaki et al. /50/.

If the reduced cobalt surface phase consists of small particles, then the observed fcc structure will be expected. The higher oxygen consumption of the promoted catalyst compared to the unpromoted containing catalyst at 298 K could be explained by the higher degrees of reduction of the promoted catalysts. If the reduced surface cobalt phase is assumed to be well dispersed, they will have a high fraction of oxidizable surface atoms. This phase is prereduced

on the promoted catalysts only, and therefore these catalysts show a relatively high oxygen consumption compared to the unpromoted catalyst. The lower oxygen consumption for the chloride containing catalyst compared to the chloride free promoted catalysts, also support that this catalyst has larger particles with a lower fraction of oxidizable surface atoms.

For the chloride free catalysts the results discussed above could indicate that reduction of the oxidic cobalt surface layer results in small particles. Then they have to be in strong interaction with the support, causing low adsorption of hydrogen and CO. This will result in a relatively large calculated mean particle size. However, the results are concerned with uncertainty, and the first explanation could also be possible for these catalysts.

4.1.3.5 Summary of the H_2 and CO adsorption measurements

- The total H_2 uptake on 9%Co/Al_2O_3 shows a slight decrease with increasing calcination temperature. This is most probably due to increased sintering of the reduced cobalt particles with increasing temperature.

- The H_2 and CO uptake on Co/Al_2O_3A increases with increasing Pt addition. This is assumed to be due to increased reduction extent of cobalt, but could also partly be due to adsorption on Pt and increased degree of spillover of H_2 and CO from Pt to support.

- The CO uptake on Re promoted Co/Al_2O_3A increases to the same amount as on Pt promoted catalyst (about three times the amount on Co/Al_2O_3A).

- The H_2 uptake increases also on Re promoted Co/Al_2O_3A, but not to the same amount as on Pt promoted Co/Al_2O_3A. Because rhenium is known /126/ for not adsorbing H_2, most of the increase in this case is assumed to be on reduced cobalt.

- The CO:H adsorption ratio on the investigated catalysts increases in the order

Co1.0Re > Co1.0Pt > Co0.5Pt > Co

- The CO:H adsorption ratio increases for the total amount of gas adsorbed compared to the amount of strongly adsorbed gas. This could be due to weakly adsorbed CO on unreduced oxidic cobalt, on $CoAl_2O_4$ or on the support.

- The chloride containing Pt promoted catalysts did not show increased H_2 adsorption compared to the unpromoted catalysts.

- The Co_3O_4 particles on the calcined, not reduced, catalysts showed from XRD measurements only small differences in size. The calculated mean particle size for the reduced cobalt phase is from the adsorption data and measurements of reduction extent found to be nearly the same for the unpromoted and the chloride free promoted catalysts. The calculated particle size for the chloride containing catalyst was larger compared to the others. The reduced cobalt on the promoted catalyst could possibly exist as both large particles generated from Co_3O_4, and as well dispersed, small particles generated from the oxidic cobalt surface layer, with high surface but also with strong interactions with the support.

4.2 Activity measurements

4.2.1 High temperature / 7 bara total pressure

Kinetic measurements were performed for unpromoted Co/Al_2O_3A and Co/Al_2O_3A promoted with platinum, rhenium and other "noble" metals, all calcined at 673 K. The experimental conditions were varied for the purpose of finding a simple power rate expression of the type

$$r_{HC} = A \cdot e^{-E/RT} \cdot P_{H_2}^{X} \cdot p_{CO}^{Y} \qquad (4\text{-}3)$$

where r_{HC} - Reaction rate
A - Preexponential factor
E - Apparent activation energy
p_{H2} - Partial pressure of H_2
p_{CO} - Partial pressure of CO

The reaction temperature was varied in the range 489 K - 529 K, the partial pressure of hydrogen in the range 2.3 - 6.8 bara, and the partial pressure of CO in the range 1.2 - 4.5 bara. Only one parameter was varied at a time, with the others kept at the "standard" values: T = 513 K, P_{H2} = 4.7 bara and P_{CO} = 2.3 bara. P_{total} was usually kept at 7 bara, but in the cases with P_{H2} = 6.8 bara, and P_{CO} = 4.5 bara, P_{total} was kept at 9 bara. When $P_{H2} + P_{CO} <$ 7 bara, helium was added, keeping the total pressure at 7 bara. The space velocity, (GHSV) was varied with the intent to keep the CO conversion between 4 - 10 %. The rate is usually given as [mol CO converted to hydrocarbons] / [gram of cobalt in catalyst · second] rather than turnover frequency. This is due to the problems in determining the dispersion of bimetallic catalysts reliably, as discussed in the previous chapter.

Figure 4-22 shows a typical reaction run plot for the cobalt catalysts. The temperature dependence of CO hydrogenation over Co/Al_2O_3A are shown in Figure 4-23. The H_2 and CO partial pressure dependencies are shown in Figure 4-24 and 4-25, respectively. In Figure 4-26 the temperature dependence of CO hydrogenation over Co/Al_2O_3A and $Co0.1Pt/Al_2O_3A$ are compared. Figure 4-27 shows a comparison of the CO conversion over the same two

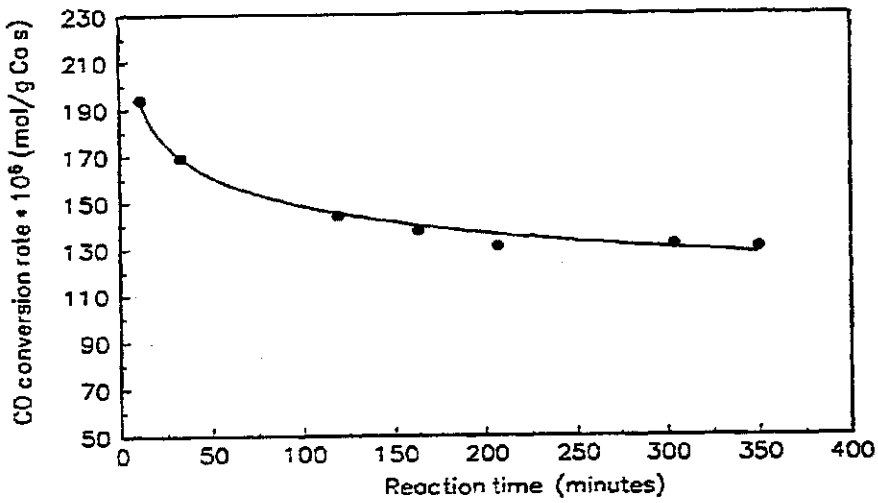

Figure 4-22. A typical reaction run plot for the cobalt catalysts. Catalyst: Co/Al_2O_3A calcined at 673 K, T = 508 K, P_{tot} = 7 bara and H_2:CO = 2.

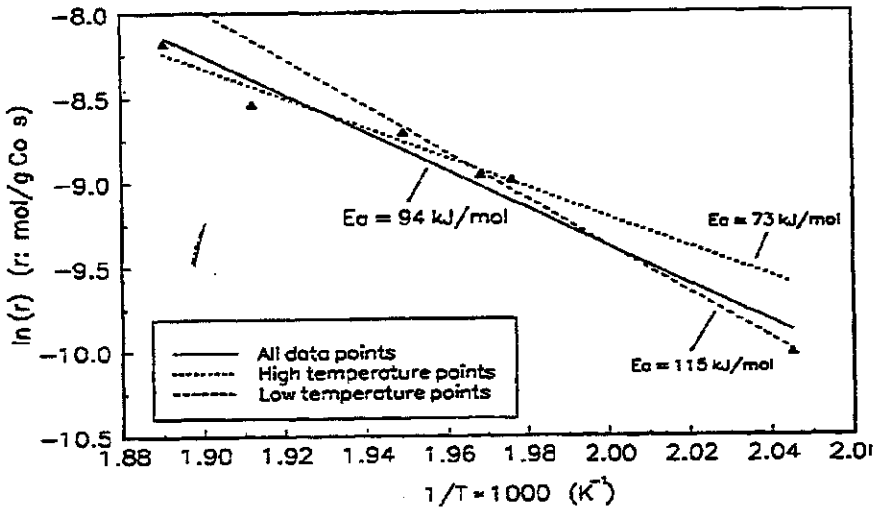

Figure 4-23. Arrhenius plot showing the temperature dependence of the CO hydrogenation rate over Co/Al_2O_3A calcined at 673K. P_{tot} = 7 bar, H_2:CO=2.

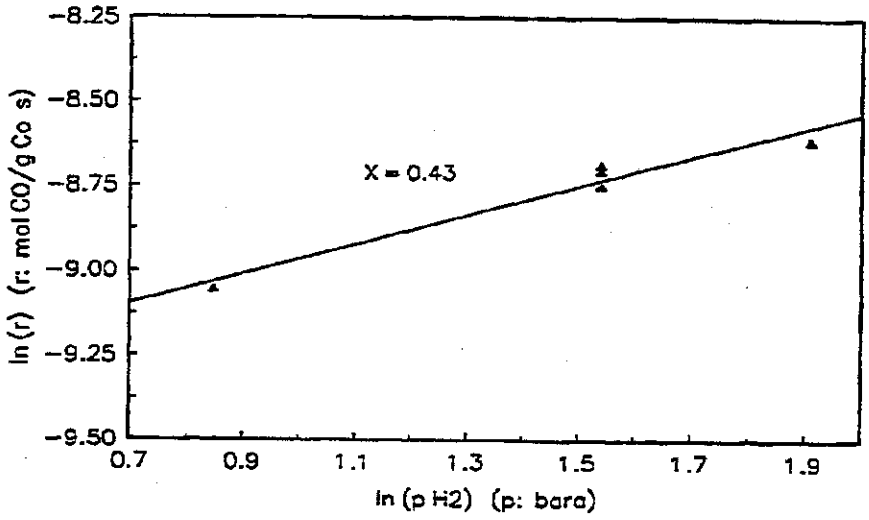

Figure 4-24. Hydrogen partial pressure dependence of the CO hydrogenation rate over Co/Al_2O_3A calcined at 673 K. P_{CO}=2.3 bar, T =513 K, P_{tot}=7 bar.

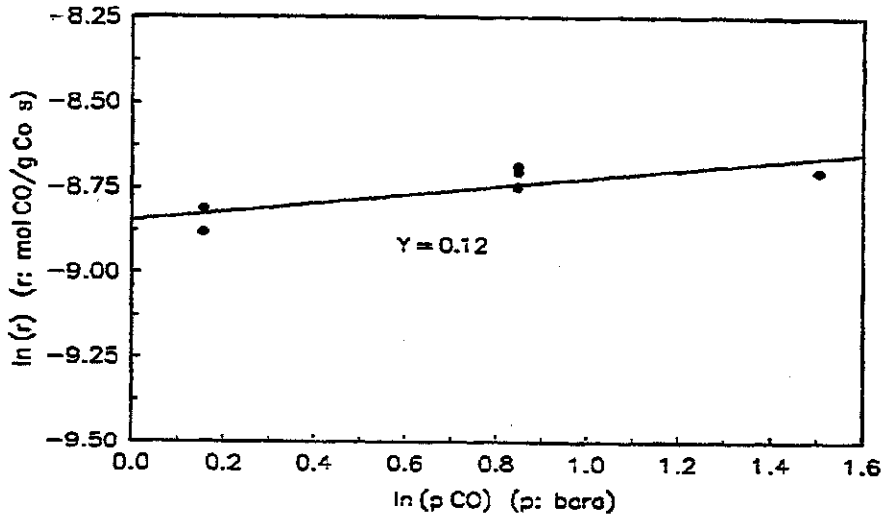

Figure 4-25. CO partial pressure dependence of the CO hydrogenation rate over Co/Al_2O_3A calcined 673 K. P_{H2} = 4.7 bar, T = 513 K, P_{tot}= 7 bar.

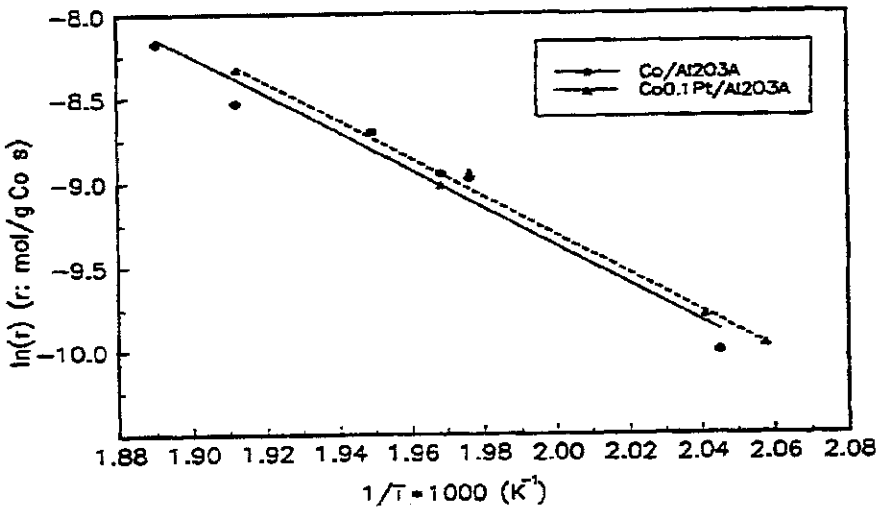

Figure 4-26. Arrhenius plot for Co/Al_2O_3A and $Co0.1Pt/Al_2O_3$. P_{tot}=7 bar, H_2:CO=2, GHSV = 56000 Nml/g cat·h.

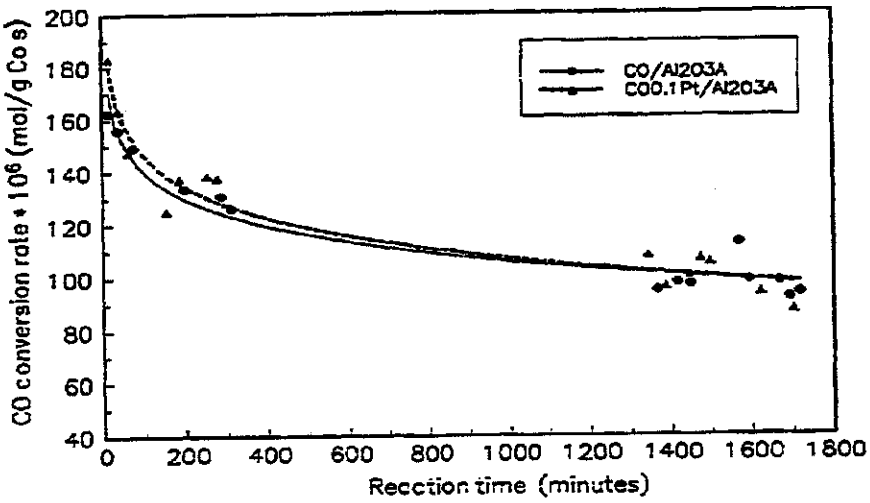

Figure 4-27. CO conversion rate over Co/Al_2O_3A and $Co0.1Pt/Al_2O_3A$, both calcined at 673 K. T = 506 K, P = 7 bara and $H_2/CO = 2$.

Table 4-13. Rate[a] as a function of promoter added to Co/Al_2O_3A calcined at 673 K. Measured after 300 minutes. T = 513 K, P_{tot} = 7 bara, H_2/CO = 2, GHSV = 56000 $Ncm^3/(g\ cat \cdot h)$.

Promoter (wt %)	Re	Pt*[b]		Ir	Rn	Pd	Unpromoted
	0.1%	0.1%	1 %	0.1 %	0.1 %	0.1 %	
Rate[a]	190	170	165	160	150	130	180

[a] CO conversion rate, (mmol/g Co·s)
[b] * denotes a chloride containing platinum precursor.

catalysts in experiments lasting for more than 1400 minutes. Table 4-13 shows the CO conversion at 513 K and 7 bara as a function of type of promoter. Formulas for calculation of rate and selectivity are shown in Appendix 6.

The experiments were normally carried out for 300 - 400 minutes, and a relatively sharp decrease in the rate appeared during the first 100 minutes. Then the rate decreased more slowly. After 300 minutes the rate had dropped to approximately 75 % of the rate measured after 25 minutes. Figure 4-27 shows run plots for "long time" runs, lasting for more than 1400 minutes. The rate is decreasing even more slowly after 1400 minutes compared to 300 minutes. The exactly course during the first 100 minutes was difficult to reproduce, and therefore the reported rates are measured after 300 minutes, unless something else is stated. When the rate is measured at the same time for all the compared catalysts, the difference in slope between 300 and 1400 minutes is considered to be unimportant in determining differences in activity between the catalysts.

The solid line shown in Figure 4-23 gives an apparent activation energy of 94 kJ/mol. Linear regression of the data points in Figure 4-24 and 4-25 gives a reaction order in H_2: X = 0.43 and in CO: Y = 0.12. The preexponential factor becomes from these data $1.8 \pm 0.3 \cdot 10^5$. The resulting rate expression will then be:

$$r_{HC} = 1.8 \cdot 10^5 \cdot e^{-94 \cdot 10^3/RT} \cdot p_{H_2}^{0.4} \cdot p_{CO}^{0.1} \qquad (4\text{-}4)$$

Table 4-13 shows only small differences in rate between catalysts with and without 0.1 wt% addition of noble metals at the "standard" conditions. The unpromoted Co/Al_2O_3A shows one of the highest activities. Higher amounts (1 wt %) of platinum do not alter this result. The parallel lines in Figure 4-26 show that also the apparent activation energy for $Co0.1Pt/Al_2O_3A$ is the same as for unpromoted Co/Al_2O_3A.

The value of the activation energy observed over Co/Al_2O_3A is somewhat lower than reported by others on comparable catalysts (Table 2-1) /30,31,32,33/. The results referred to in Table 2-1 are measured at lower temperature and/or lower pressure, giving lower reaction rates. These measurements will therefore not be affected by eventual reactant diffusion limitations in the same degree as the measurements presented here. If such limitations occur they will be more important with increasing rates, and this will be seen on the Arrhenius plot as a deviation from the theoretical straight line. If only values from the high temperature range is used (dotted line in Figure 4-23), the apparent activation energy will be 73 kJ/mol. If only the experiments at the lowest temperatures (the dashed line in Figure 4-23) are used for determination of the activation energy, it is measured to be 115 kJ/mol. The low temperature value is more in agreement with literature values /6,30,32,142/ than the value from the entire or the high temperature range.

The reaction order for CO is reported /6,31,34,142/ to be between 0 and -1.0. The corresponding values for H_2 are positive, and between 0.5 and 1.5. In this investigation the reaction order with regard to both CO and H_2 is positive, and between 0 and 0.5. In both cases (Figure 4-24 and 4-25) the slope is decreasing with increasing pressure.

Promotion with noble metal as platinum and rhenium has, as seen from TPR analyses and chemisorption measurements, resulted in higher degrees of reduction of the catalysts and higher amounts of adsorbed gas. In view of this it was surprising not to find significant differences in activity between the promoted and the unpromoted catalysts. As seen in Table 4-13 only small differences in catalyst activity are observed after promotion with various noble metals. In addition, there is no correlation between the activities shown in Table 4-13 and the previously shown ranking of the ability of the different promoters to facilitate the cobalt reduction.

Several different phenomena should be mentioned as possible explanations to the observed decrease in the CO conversion rate, and to the lack of difference in activity between the unpromoted and the promoted catalysts. The different phenomena will be discussed as though no other effects occur simultaneously:

I) Wax condensation in the catalyst pores. Huff and Satterfield /74/ calculated the rate of condensation of high molecular weight products in the catalyst pores. They simulated CO hydrogenation over iron catalysts. Their results show that the time required to fill the first pore will decrease with both increasing pressure and temperature, due to the increase in intrinsic reaction rate. Increasing pressure will also give increased condensation, which further reduces the time required to fill the first pore. The presence of wax products in the pores will lead to a decreased concentration of the reactants at the catalyst surface because of the limited solubility of the reactants in the liquid products.

II) Reactant diffusion limitations. If the reactant mass transfer (diffusion) to the catalyst surface is slower than the reactant consumption in the reaction, the reaction rate will be diffusion controlled. Both bulk diffusion (diffusion across a boundary layer of stagnant gas near the catalyst surface) and Knudsen diffusion (into narrow (< 1000 Å) pores) may be important. Bulk diffusion can be recognized by changing the catalyst loading, while keeping the space velocity constant. If bulk diffusion is not important the activity/g catalyst will not be changed. Knudsen diffusion can be checked by measuring the activation energy E_a over a range of temperatures. If diffusion is important E_a changes to $E_a/2$ with increasing temperature /138/. Another result of Knudsen diffusion limitation is that the reaction order for the limited reactants changes from n to (n+1)/2 with increasing degree of limitation.

CO hydrogenation experiments done over Co/Al_2O_3A in a micro balance at NTH /128/ can be used in calculation of the extent of porefilling. At 523 K the weight increase during the first 50 minutes is 30 mg/g catalyst and during the first 300 minutes 55 mg/g catalyst. As an estimate 100 % of the weight increase is considered to be due to wax formation. Then, with a pore volume of 0.4 cm^3/g (Appendix 5) the weight increase after 300 minutes corresponds

to an extent of wax filling of approximately 20 %. This should be enough to form a liquid film over the catalyst resulting in diffusion limitations. Narrow pores could be "closed" by a wax film at the pore outlet, giving a pronounced effect even with a very low degree of filling. The relatively slow deactivation rate observed after 300 minutes could from the calculated 20 % porefilling be due to a further filling of the large pores by wax. However, some of the observed weight increase is most likely due to carbide and hydroxyl formation, and this will give a lower extent of waxfilling. Still, the effect is assumed to be unchanged.

Gas phase diffusion is much faster than liquid diffusion. Then it is obvious that diffusion limitations is more probable as wax products remains in the pores. Certainly, the first analysis is taken 10 to 20 minutes after the temperature has reached 513 K, and the reaction was started up at 463 K 50 minutes earlier. The CO conversion rates are lower, but the chain growth probability is larger at lower temperatures. Even at the time for the first analysis there might therefore be a possibility for wax present in the pores. Then the reaction rate over the promoted catalysts (and eventually the unpromoted catalyst) could be diffusion limited, and this will explain the lack of difference between the promoted and the unpromoted catalysts. The wax products will gradually fill the pores, and the rate will decrease correspondingly /75.81/. When the pores are completely filled by wax the rate will stabilize at a certain level.

The dotted and dashed lines in Figure 4-23 indicate that there is a possibility for reactant diffusion controlled reaction rates. The apparent activation energy is decreasing from 115 to 73 kJ/mol with increasing temperature. The reaction order for CO is higher than expected from literature values. This could indicate that CO is the limited reactant in these investigations.

Post et al. /4/ investigated the extent of diffusion limitations in the Fischer-Tropsch reaction at temperatures between 473 and 523 K over catalyst particles in the size range 0.2 - 2.6 mm, and with pore diameters in the range 100 - 1000 Å. By use of the Thiele model for diffusion limitations, and H_2 diffusion data, they found evidence for retardation of the reaction rates due to liquid-filled pores. In the present investigation both particle size and pore radius are lower (0.075 - 0.3 mm and 30 - 60 Å, respectively). The Thiele modulus is dependent on both these properties ($R_{particle}^2/r_{pore}$), and it is therefore possible from the results reported by

Post et al. /4/ to suggest that diffusion limitations due to wax in the pores could be present also in this study.

Iglesia et al. /81/ criticize the model used by Post et al. /4/ for the choice of hydrogen as the diffusion limited reactant. Their selectivity and rate data, as well as independent CO and H_2 diffusivity and solubility measurements, suggest that CO is the diffusion-limited reactant for feeds with H_2 : CO > 1.6. The same is indicated in the present investigation as discussed above.

III) Reoxidation of cobalt. Roynek and Polansky /17/ found a decreased Co^0/Co^{2+} ratio on uncalcined, chloride-derived Co/SiO_2 catalysts after four hours CO hydrogenation compared to the ratio prior to H_2/CO exposure. Both nitrate- and acetate-based catalysts displayed slight increases in Co^0 content after H_2/CO exposure. The chloride-based catalyst showed high degree of reduction (65 %) before reaction, while the nitrate- and acetate-based catalysts showed low degrees of reduction (9 % and 18 %, respectively). The decrease in Co^0/Co^{2+} ratio was suggested to be due either to partial reoxidation of reduced cobalt by water formed during H_2/CO reaction and /or to partial blockage of surface Co^0 sites by carbon deposited during CO disproportionation. The catalysts in this study are nitrate-derived, but the support are alumina, which interacts with cobalt in a different way than silica /79/. The extent of reduction of Co/Al_2O_3A is much higher (about 35 %) compared to the uncalcined, nitrate-based Co/SiO_2. It could therefore be suggested that product water might reoxidize reduced cobalt atoms on alumina to form an inactive cobalt phase. This will result in a decrease in the observed rate.

Reoxidation of the reduced cobalt on unpromoted and promoted catalysts may be observed in different ways, dependent of the cobalt particle size distribution present on the support surface.

First, it can be assumed that all cobalt particles are of the same size; as relatively large particles, interacting weakly with the support. Reoxidation will in this case take place on both promoted and unpromoted catalysts to the same extent. This will be observed as a decrease

in activity, but there will be a difference in activity between the promoted and the unpromoted catalysts, due to the larger amount of reduced cobalt on the promoted catalysts.

Second, it can be assumed large "bulky" particles combined with small particles interacting strongly with the support. Then the well dispersed cobalt from reduction of the oxidic cobalt layer on the promoted catalysts could be assumed to reoxidize faster than the cobalt from the larger crystalline Co_3O_4 particles. This will give an increase in the slope of the CO conversion curve for the promoted catalysts compared to the unpromoted catalyst, containing only large cobalt particles. If the reoxidation of the surface cobalt layer is very fast, this might occur before the first analysis is taken. This can explain the lack of difference in activity between the promoted and the unpromoted catalysts. A further oxidation of the large particles will then be as described above in the first case, but without a difference in the activity. A slow reoxidation of the surface cobalt is not probable from the observed coincidence in the slope of the CO conversion curve for the two catalysts.

IV) Sintering of the metallic cobalt induced by product water. The water content in the reducing gas is an important factor for the dispersion of the reduced metal /120/. Increasing water content gives sintering and decreased dispersion. It is also commonly observed that water vapor enhances the rate of sintering of high area catalysts during reaction /55/.

Sintering must also be discussed in view of the probable metal particle size distribution on the support. The observed effects of sintering will be much like the effects of reoxidation: Only large particles present on the surface will give increased rate to both the unpromoted and the promoted catalysts, while a difference in activity will be observed. If well dispersed particles are present, they may sinter fast. Then it is impossible to separate this case from the case where all the particles are large immediately after the reduction. The observed result in use of the catalysts will be the same: A difference in activity will be present between the catalysts, corresponding to the increased degree of reduction for the promoted catalysts.

If the sintering of the well dispersed phase is slow, the observed effect will depend on the activity rates on this phase. If strong interactions with the support is present, as discussed in

Chapter 4.1.3.4. the activity is probably low. Then sintering of this phase would be less important: The metal phase looses surface area, but as it becomes more "bulky" it may be assumed to increase the activity due to weaker interaction with the support.

On the other hand, if the activity on a well dispersed cobalt phase is high, the sintering of this phase will give increased decrease in the activity compared to the decrease in activity over the unpromoted catalyst.

From this sintering could consequently be suggested to explain the decrease in activity, but not the lack of difference between the promoted and the unpromoted catalysts.

V) Deposition of carbon and carbonaceous materials. Carbon on the surface from dissociated CO can either be hydrogenated and form the desired products, or carbon diffusion into the cobalt lattice and formation of inactive cobalt carbide may take place. Carbon diffusion can be regarded as a competing reaction to hydrogenation and chain growth, depending of the hydrogenation rate.

The carbidic carbon on surface may also polymerize to chains of insoluble carbonaceous deposits (graphitic carbon), poisoning the metallic surface /140/.

But neither formation of graphitic carbon nor cobalt carbide /55,140/ is reported to be present at standard Fischer-Tropsch conditions during the initial period investigated in this study. Nakamura et al. /139/ deposited carbon on 6 %Co/Al_2O_3 by the Boudouard reaction at 500 K. By reaction with hydrogen at 353 - 493 K, and the use of ^{13}C and D isotopes, they could observe predominantly reactive carbidic carbon, but also highly active CH and CH_2 species. Carbidic carbon was only decomposed to graphitic carbon when the deposition temperature was raised to 700 K, but even at this temperature a certain amount of carbidic carbon was found to remain on the surface.

Johnson et al. /44/ have recently studied the effect of surface structure on the CO hydrogenation by comparing the steady state activity and selectivity of submonolayer cobalt deposited on W(100) and W(110) with those of carbonyl-derived Co/Al_2O_3 of varying

dispersion and extent of reduction. Enhanced CO dissociation ability of low coordination sites was expected to cause poisoning by graphite or by a high surface carbide level. After reaction, Co/W surfaces showed high coverage of both carbon and oxygen with AES carbon lineshapes characteristic of carbidic carbon. But no graphite was formed under low temperature (475-525 K) reaction conditions in the investigations done by Johnson et al.

Guczi et al. /49/ suggested that a decrease in activation energy as a result of iridium addition to alumina supported cobalt catalysts, could be a result of decrease in carbide formation. Correspondingly, a constant activation energy for different ruthenium/platinum catalysts was interpret as a absence of carbon deposit, due to the presence of platinum with high coverage of hydrogen. If these conclusions is used on the result presented in Figure 4-26, it could be suggested that no deactivation takes place due to carbonaceous materials.

From the literature referred to above it is not likely that the initial decrease in activity, or the lack of difference between the catalysts is due to a decreased number of active catalytic sites caused by graphitic carbon or cobalt carbide formation. However, the slow decrease in rate observed between 300 and 1400 minutes could partly be due to formation of these species.

The different discussions show that the observed initial (0 - 300 minutes) decrease in the CO conversion rate can be explained by

- waxfilling of the pores and diffusion limitations in the liquid products.
- reoxidation of reduced cobalt metal and/or
- sintering of the reduced metal.

Insoluble carbonaceous deposition is only suggested to be a probable explanation for the more slow decrease in rate with increasing reaction time.

The lack of the expected difference in activity between the promoted and the unpromoted catalyst is probably caused by

- reactant diffusion limitations or
- a rapid reoxidation of the reduced surface cobalt layer, caused by product water.

Of course, if several of these effects occur simultaneously one effect may disguise another.